Note on Earhtquake Seismology <4> Numerical models

Hideo Aochi

1. Quantitaive Framework
2. Crack theory and fracture
3. Friction and rupture growth
4. Numerical models
5. Earthquake scaling
6. Obsevational seismology

4 Janueary 2026

Mechanical point of view

1. Equation of motion of the medium $\rho\ddot{u} = \nabla \cdot \tau$

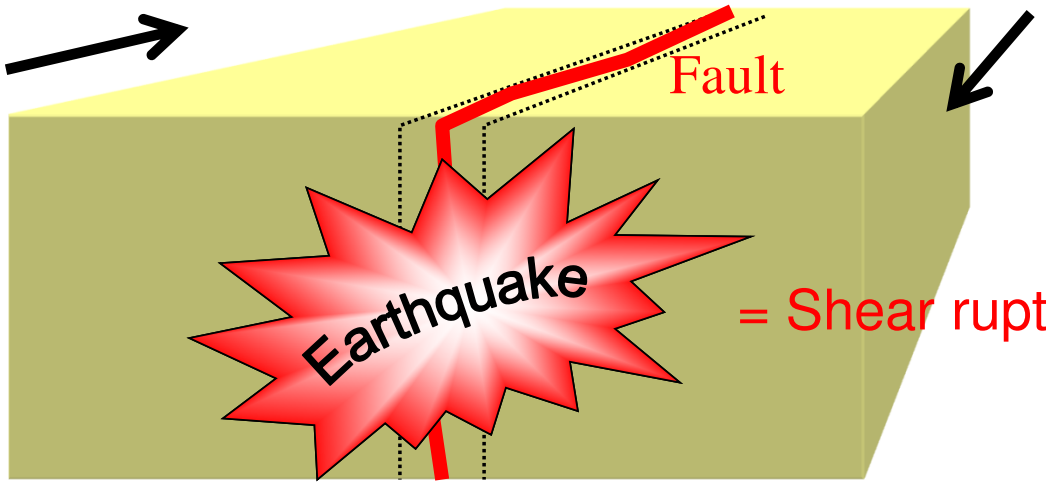

= Shear rupture

3. Initial Condition (Loading)

$\tau = \tau_0$

2. Boundary condition (Friction) $\tau = \tau(\Delta u, \Delta \dot{u}, t, T, \cdots)$

Field earthquake (M7)	**30 km**	**>1 m**	**~10 MPa**	**m/s**	**km/s**
	Dimension	***Slip***	***Stress***	***Slip rate***	***Rupture velocity***
Laboratory	**<10 cm**	**<mm**	**1-100MPa**	**m/s**	**km/s**

Geophys. J. R. astr. Soc. (1977) **50**, 643–668

A numerical study of two-dimensional spontaneous rupture propagation

Shamita Das and Keiiti Aki *Department of Earth and Planetary Sciences, Massachusetts Institute of Technology, Cambridge, Massachusetts 02139, USA*

Received 1977 February 14; in original form 1976 November 12

Summary. We present a numerical technique to determine the displacement and stress fields due to propagation of two-dimensional shear cracks in an infinite, homogeneous medium which is linearly elastic everywhere off the crack plane. Starting from the representation theorem, an integral equation for the displacements inside the crack is found. This integral equation is solved by a method proposed by Hamano for various initial and boundary conditions on the crack surface. We verified the accuracy of our numerical method by comparing it with the analytical solution of Kostrov, and the numerical solution of Madariaga. A critical stress-jump across the tip of a crack (between a grid-point inside the crack and a neighbouring point outside the crack) is used as our fracture criterion. We find that our critical stress-jump is the finite difference approximation to the critical stress-intensity factor used in Irwin's fracture criterion.

For an in-plane shear crack starting from the Griffin critical length and controlled by the above fracture criterion, the propagation velocity of the crack-tip is found to be sub-Rayleigh or super-shear depending on the strength of the material (given by the critical stress-jump) and the instantaneous length of the crack. In fact, the crack-tip velocity may even reach the *P*-wave velocity for low-strength materials. Additionally we find that once the crack starts propagating, it accelerates rapidly to its terminal velocity, and that the average rupture velocity over an entire length of fault cannot be much smaller than the terminal velocity, for smooth rupture propagation.

3 Numerical method of solving the integral equation

The integral equations that we have to solve in the case of the in-plane and the anti-plane shear crack are both of the form

$$u(x_1, 0, s) = \int\int_S \tau(x, t) g(x_1 - x, 0, s - t)\, dx dt \qquad (14)$$

e.g. Kostrov (1966)

where u is the appropriate component of displacement, g the appropriate component of the Green's function and $\tau(x, t)$ the traction on the crack.

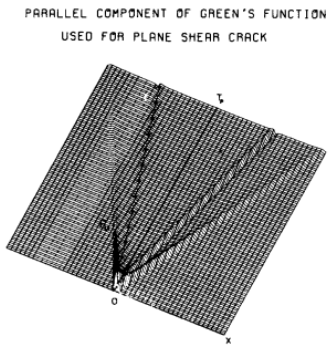

Figure 4. Composite plot showing the discretized kernel $F_{11}(X, T_p)$ giving the parallel component of the Green's function for the in-plane problem. The *P* waves and Rayleigh waves are clearly visible. $F_{11}(X, T_p)$ is symmetric about $X = 0$.

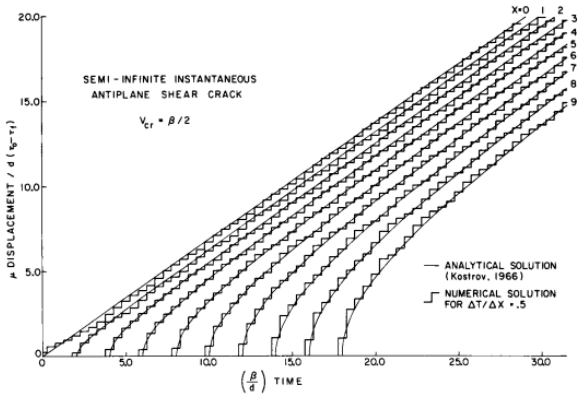

Figure 6. Comparison of analytical solution due to Kostrov (1966) with our numerical solution for a semi-infinite instantaneous anti-plane shear crack extending at half the shear-wave velocity.

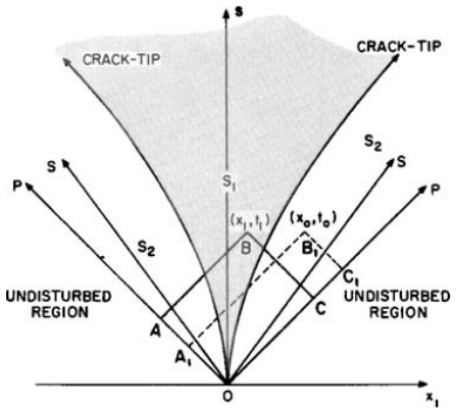

Figure 2. Trajectory of the crack-tip in the $(x - s)$ plane. S_1 is the crack region and S_2 is the region outside the crack. P and S denote P and S waves from the initial point of break.

$$u(x_1, s) = \iint_S \tau(x,t) g(x_1 - x, s - t) dx dt$$

$$u_n(x_i, t_k) = \Delta t \Delta x \sum_{j,l} F(x_i - x_j, t_k - t_l)\tau(x_j, t_l)$$

where $F(x_j, t) = \frac{1}{d}\int_{x-d/2}^{x+d/2} g(y,t)dy$

$u_n(x_i, t_k) = 0$ on S_2 ⇒ $\sum_{j,l} F(x_i - x_j, t_k - t_l)\tau(x_j, t_l) = 0$

$$F(0,0)\tau(x_i, t_k) + \sum_{j \neq i, l \neq k} F(x_i - x_j, t_k - t_l)\tau(x_j, t_l) = 0$$

unknown known

$u_n(x_i, t_k) \neq 0$ on S_1 ⇒ $\tau(x_i, t_k) = \mathrm{f}(u_n(x_i, t_k), \dot{u}_n(x_i, t_k))$ Friction, constitutive law

VOL. 82, NO. 36 JOURNAL OF GEOPHYSICAL RESEARCH DECEMBER 10, 1977

Fault Plane With Barriers: A Versatile Earthquake Model

SHAMITA DAS[1] AND KEIITI AKI

Department of Earth and Planetary Sciences, Massachusetts Institute of Technology Cambridge, Massachusetts 02139

Shear cracks with finite cohesive forces can propagate by skipping past barriers. The barriers left behind may remain unbroken or may eventually break because of subsequent increase in dynamic stress depending on the ratio of barrier strength to tectonic stress. This model can explain a variety of observations on rupture in the earth, including (1) segmentation of the fault or ruptured zone in earthquakes and rock bursts, (2) ripples in seismograms which cannot be explained by path effect, and (3) departure of the scaling law of the seismic spectrum from that based upon the similarity assumption. The model also explains why the simple uniform dislocation model sometimes works better than the crack model without barriers. It also predicts, contrary to common belief, that an earthquake with low average stress drop may generate relatively greater amounts of high-frequency waves than an earthquake with high average stress drop. One important consequence of our barrier model is the possibility of predicting the occurrence of aftershocks by analyzing the source spectrum of the main shock.

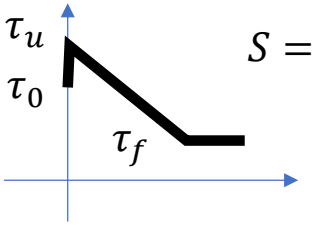

$$S = \frac{\tau_u - \tau_0}{\tau_0 - \tau_f}$$

$$1 + S = \frac{\tau_u - \tau_f}{\tau_0 - \tau_f} = \frac{ck_c}{(\tau_0 - \tau_f)\sqrt{d}}$$

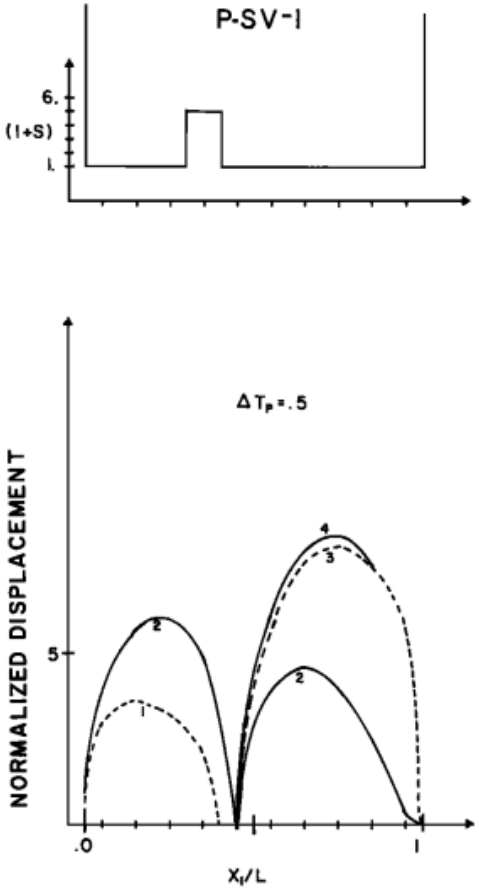

Fig. 2. Case P-SV-1, in which one barrier exists on the fault plane. See Figure 1 legend for details. The crack tip skips the barrier without breaking it.

Boundary Integral Equation Method

$$u_i(\vec{x},t) = \int_0^t d\tau \int_\Sigma d\Sigma \Delta u_j(\vec{\xi},\tau) c_{jkst} \nu_k \frac{\partial G_{is}(\vec{x},t-\tau;\vec{\xi},0)}{\partial \xi_t}$$

Representation Theorem (Aki and Richards, 1980)

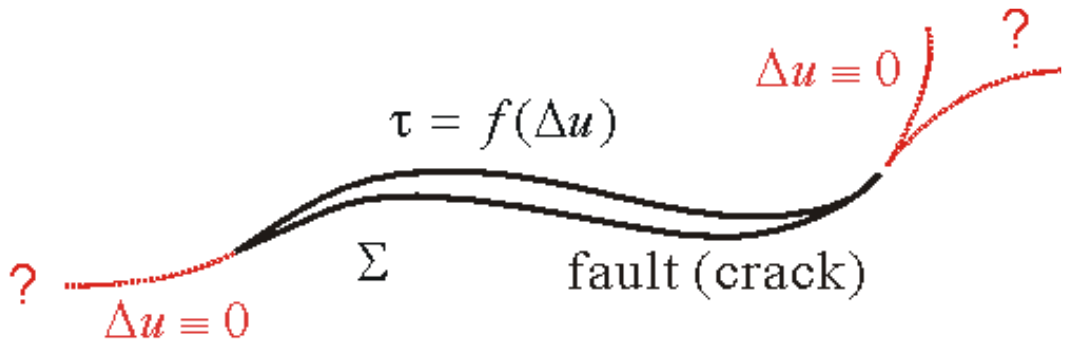

- Stress / Displacement expression
- Time / Fourier domain
- Real space / Wave number

cf. Koller et al. (1992), Cochard & Madariaga (1994), Fukuyama & Madariaga (1995)…

Coordinate system for formulation

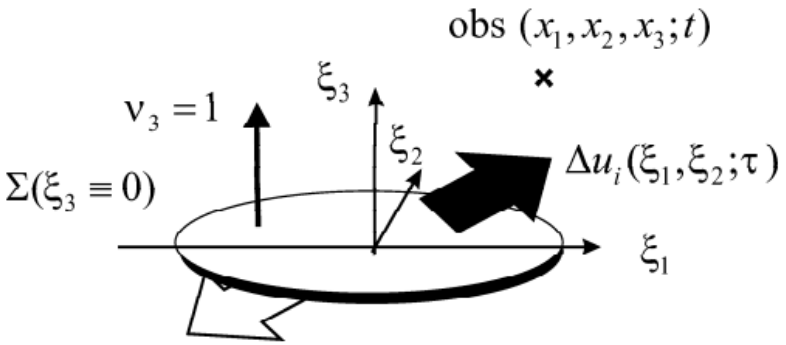

$$\gamma_i = \frac{x_i - \xi_i}{r}$$

$\Delta u_1, \Delta u_2$: shear
Δu_3: tensile

Figure 2.2: The coordinate system where a planar fault is embedded on $x_3 = 0$. Slip discontinuity Δu_ζ occurs on the fault.

$$\tau_{pq}(\boldsymbol{x}, t) = -\int_0^t \int_\Sigma \Delta u_j(\boldsymbol{\xi}, \tau) c_{j3st} c_{pqin} \frac{\partial^2}{\partial x_n \partial x_t} G_{is}(\boldsymbol{r}, t - \tau) d\Sigma d\tau,$$

$$
\begin{aligned}
\tau_{3\eta}(\boldsymbol{x},t) = &-\frac{\mu}{4\pi\beta^2}\int \frac{1}{r}\Delta\ddot{u}_\eta(\boldsymbol{\xi},\|t-\frac{r}{\beta}\|)d\Sigma \\
&-\frac{\mu}{4\pi}\int \frac{1}{r^2}\Bigg[12\frac{\beta^2}{r^2}\int_{r/\alpha}^{r/\beta} t'\Big(\gamma_\eta\Delta u_{\zeta,\zeta}(\boldsymbol{\xi},\|t-t'\|)+3\gamma_3\Delta u_{3,\eta}(\boldsymbol{\xi},\|t-t'\|)\Big)dt' \\
&\qquad+\Big(4p^2\gamma_\eta\Delta u_{\zeta,\zeta}(\boldsymbol{\xi},\|t-\frac{r}{\alpha}\|)-2(1-8p^2)\gamma_3\Delta u_{3,\eta}(\boldsymbol{\xi},\|t-\frac{r}{\alpha}\|)\Big) \\
&\qquad-\Big(5\gamma_\eta\Delta u_{\zeta,\zeta}(\boldsymbol{\xi},\|t-\frac{r}{\beta}\|)-\gamma_\zeta\Delta u_{\eta,\zeta}(\boldsymbol{\xi},\|t-\frac{r}{\beta}\|)+14\gamma_3\Delta u_{3,\eta}(\boldsymbol{\xi},\|t-\frac{r}{\beta}\|)\Big) \\
&\qquad-\frac{r}{\alpha}2(1-2p^2)\gamma_3\Delta\dot{u}_{3,\eta}(\boldsymbol{\xi},\|t-\frac{r}{\alpha}\|) \\
&\qquad-\frac{r}{\beta}\Big(\gamma_\eta\Delta\dot{u}_{\zeta,\zeta}(\boldsymbol{\xi},\|t-\frac{r}{\beta}\|)-\gamma_\zeta\Delta\dot{u}_{\eta,\zeta}(\boldsymbol{\xi},\|t-\frac{r}{\beta}\|)+2\gamma_3\Delta\dot{u}_{3,\eta}(\boldsymbol{\xi},\|t-\frac{r}{\beta}\|)\Big)\Bigg]d\Sigma \\
&-\frac{\mu}{4\pi}\int \frac{\gamma_3^2}{r^2}\Bigg[-60\frac{\beta^2}{r^2}\int_{r/\alpha}^{r/\beta} t'\Big(\gamma_\eta\Delta u_{\zeta,\zeta}(\boldsymbol{\xi},\|t-t'\|)+\gamma_3\Delta u_{3,\eta}(\boldsymbol{\xi},\|t-t'\|)\Big)dt' \\
&\qquad-24p^2\Big(\gamma_\eta\Delta u_{\zeta,\zeta}(\boldsymbol{\xi},\|t-\frac{r}{\alpha}\|)+\gamma_3\Delta u_{3,\eta}(\boldsymbol{\xi},\|t-\frac{r}{\alpha}\|)\Big) \\
&\qquad+24\Big(\gamma_\eta\Delta u_{\zeta,\zeta}(\boldsymbol{\xi},\|t-\frac{r}{\beta}\|)+\gamma_3\Delta u_{3,\eta}(\boldsymbol{\xi},\|t-\frac{r}{\beta}\|)\Big) \\
&\qquad-4p^2\frac{r}{\alpha}\Big(\gamma_\eta\Delta\dot{u}_{\zeta,\zeta}(\boldsymbol{\xi},\|t-\frac{r}{\alpha}\|)+\gamma_3\Delta\dot{u}_{3,\eta}(\boldsymbol{\xi},\|t-\frac{r}{\alpha}\|)\Big) \\
&\qquad+4\frac{r}{\beta}\Big(\gamma_\eta\Delta\dot{u}_{\zeta,\zeta}(\boldsymbol{\xi},\|t-\frac{r}{\beta}\|)+\gamma_3\Delta\dot{u}_{3,\eta}(\boldsymbol{\xi},\|t-\frac{r}{\beta}\|)\Big)\Bigg]d\Sigma
\end{aligned}
\tag{2.46}
$$

Discretization

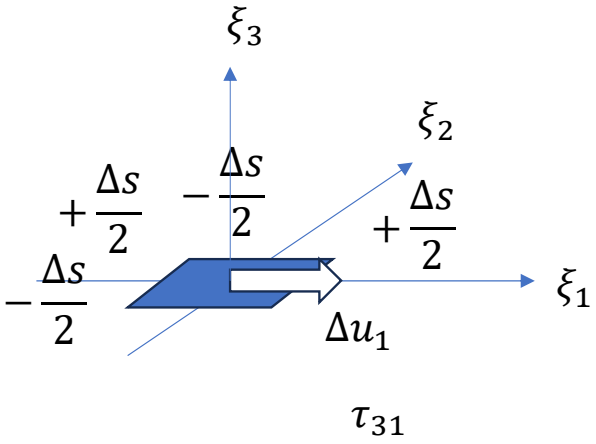

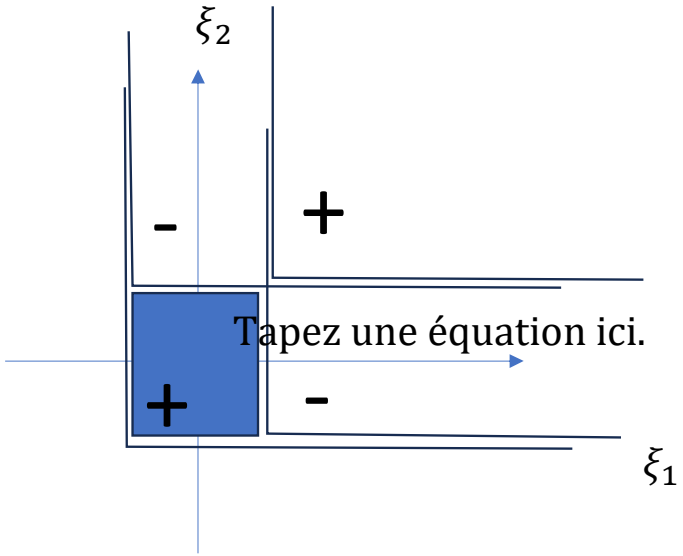

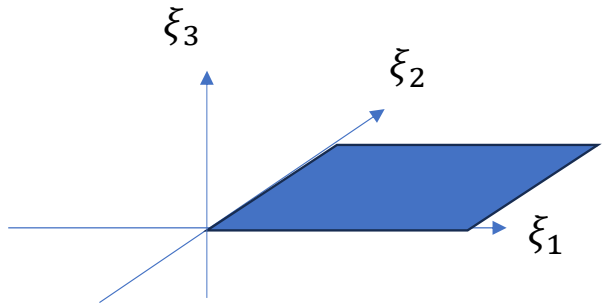

Tapez une équation ici.

$$\Delta\dot{u}_1 = V_1 \cdot H(\xi_1)H(\xi_2)H(\tau)$$

Slip rate constant on a subfault during a step

All termes are analytically integrable.

$$\begin{cases} (\text{I-}c)_{\bar{\zeta}} & x_{\bar{\zeta}} < -X_\zeta(c) \text{ for } X_\zeta(c)^2 > 0 \text{ , or } X_\zeta(c)^2 \leq 0 \\ (\text{II-}c) & \chi^2 < c^2t^2 \\ (\text{III-}c)_{\bar{\zeta}} & x_{\bar{\zeta}} > X_\zeta(c) \text{ for } X_\zeta(c)^2 > 0 \end{cases}$$

$$\chi'^2_\zeta = x_\zeta^2 + x_3^2,\ X_\zeta(c) = \sqrt{c^2t^2 - \chi'^2_\zeta} \text{ and } \chi^2 = x_1^2 + x_2^2 + x_3^2$$

Discretization (2D)

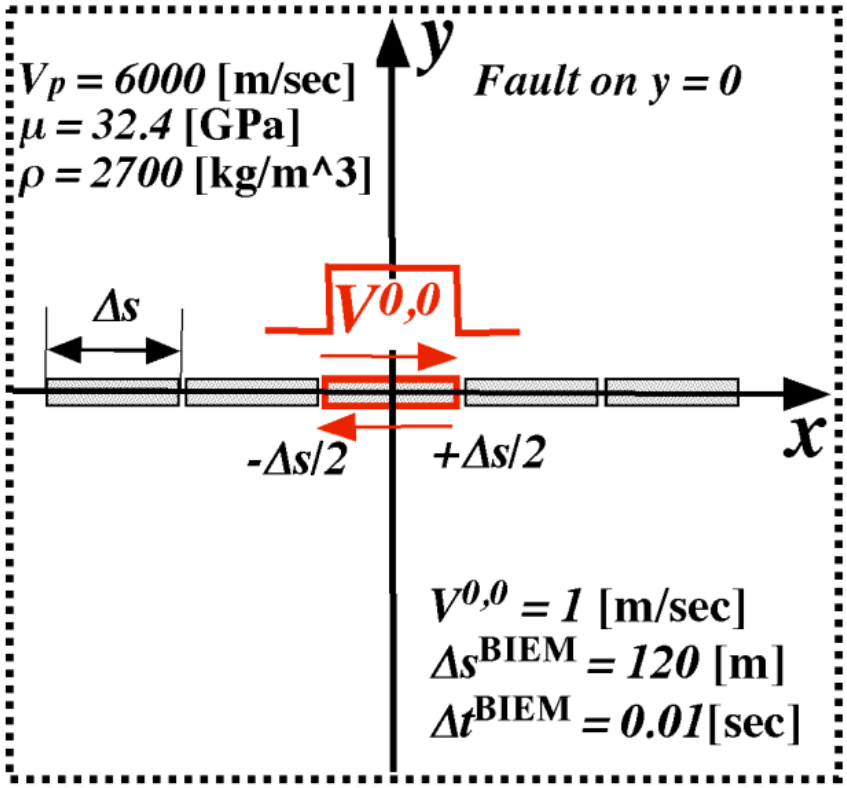

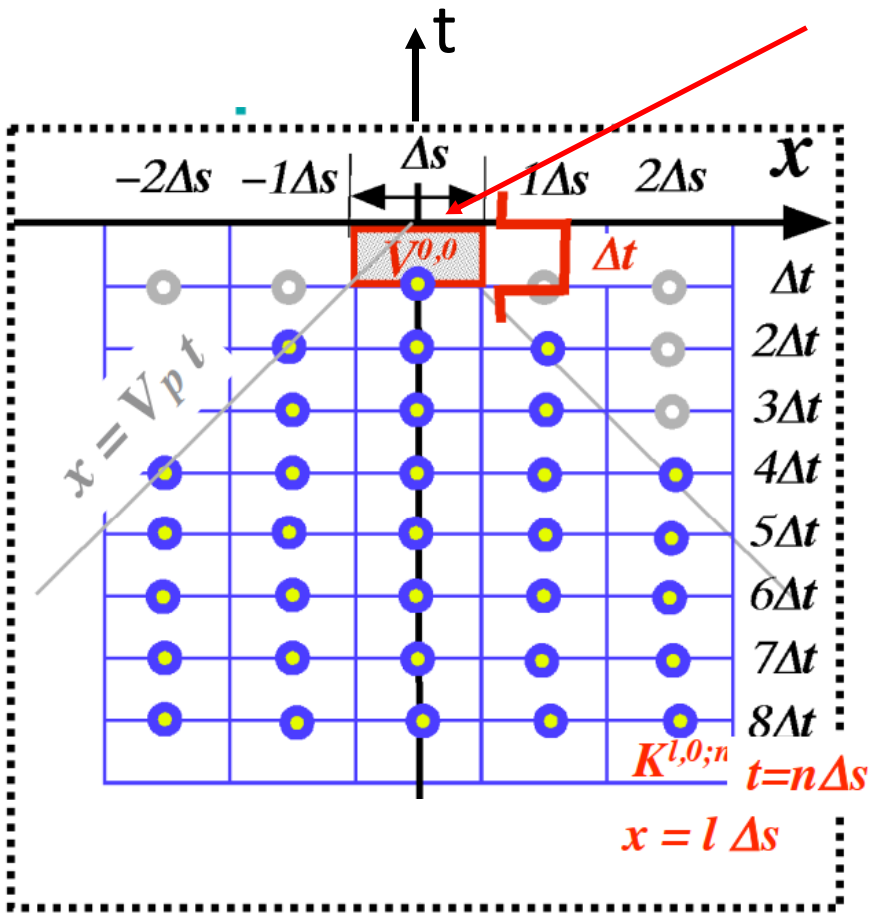

Discretization (2D)

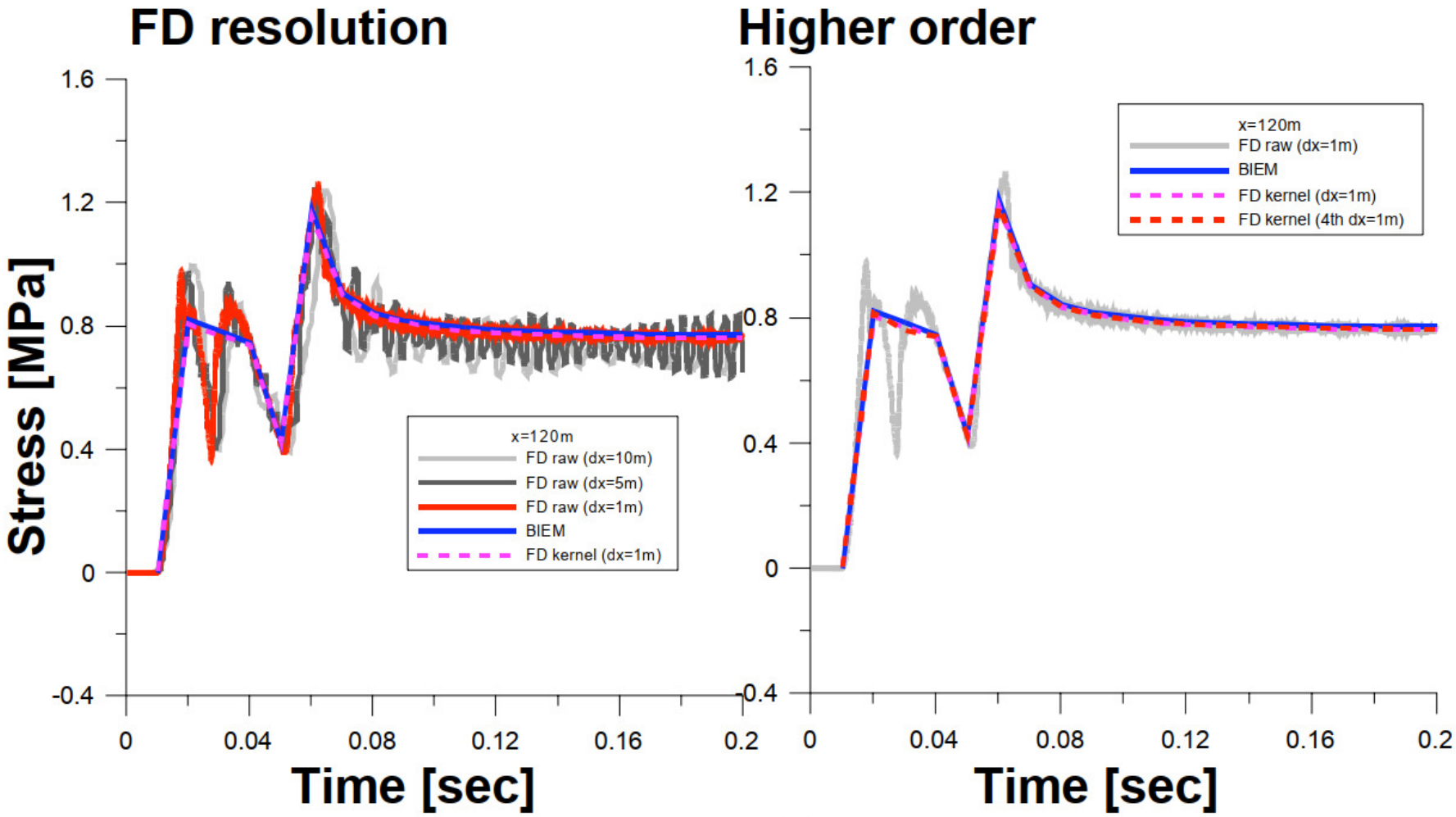

Kame, Aochi, et al. (no published work)

Result 1b: Comparison of $K^{l,0;n}$

BIEM

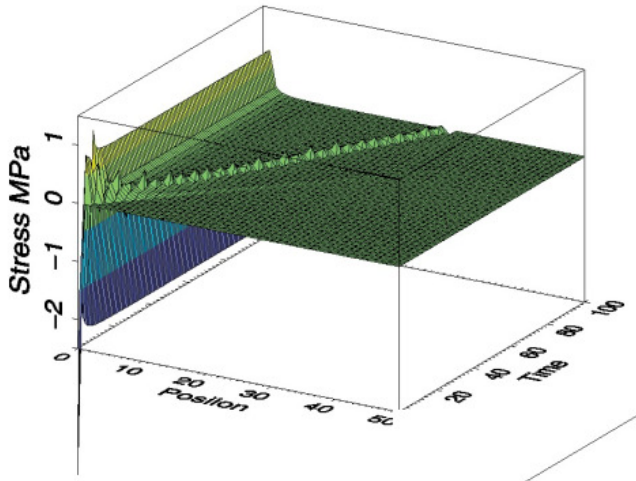

FDM kernel (1m,2nd)

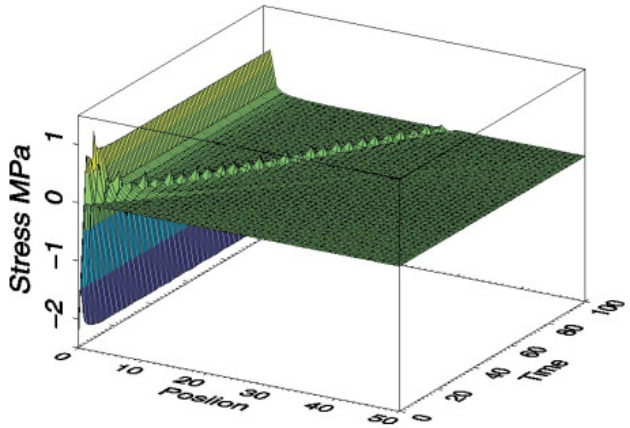

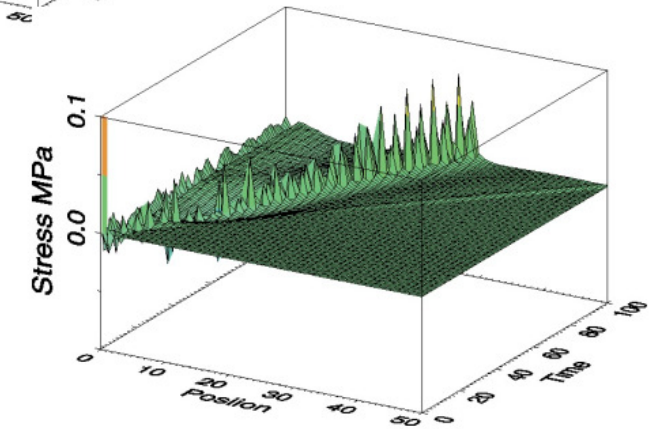

Difference FD-BIEM (x10 scale)

BIEM

$$\Delta \dot{u}_\eta(\xi_1,\xi_2,\tau) = \sum_{l,m,n} V_\eta^{lmn} \underbrace{d(\xi_1,\xi_2,\tau;\xi_1^{\,l},\xi_2^{\,m},\tau^n)}_{\text{box-like function}}$$

Typical formation of discrete BIE

$$\tau^{ijk} = \underbrace{P^{000:000} V^{ijk}}_{\text{current time step}} + \underbrace{\sum_{n=1}^{k-1} \sum_{l,m} P^{ijk:lmn} V^{lmn}}_{\text{past history}}$$

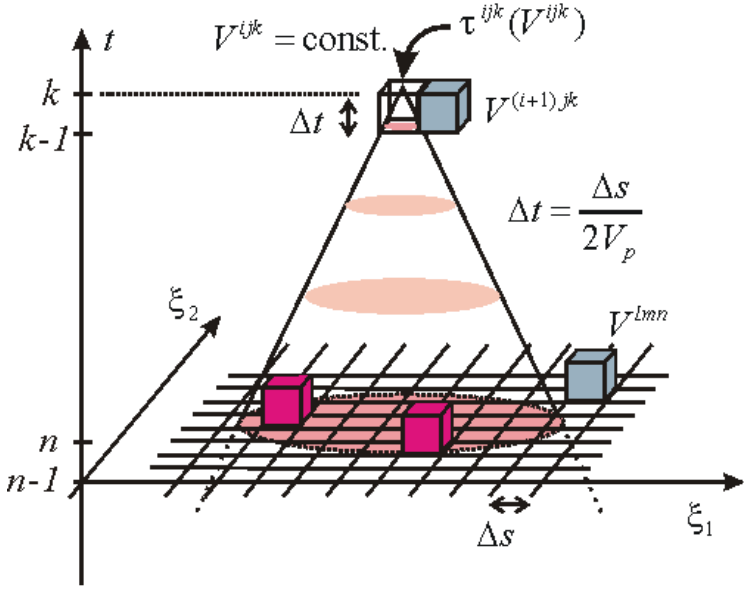

Illustration of convolution for 3D planar fault

- A simple scalar equation : y = Ax + B
- The spontaneous term (current time step) independent from past history and other grids = Explicit

With a linear slip-weakening law

BIEM $$\tau^{ijk} = P^{000}V^{ijk} + \sum_{n=1}^{k-1}\sum_{l,m} P^{ijk:lmn}V^{lmn}$$

Slip-weakening $$\sigma^{ijk} = \sigma^{ij(k-1)} - aV^{ijk}\Delta t$$

$$P^{000}V^{ijk} + \sum_{n=1}^{k-1}\sum_{l,m} P^{ijk:lmn}V^{lmn} = \sigma^{ij(k-1)} - aV^{ijk}\Delta t$$

$$(P^{000} + a\Delta t)V^{ijk} = \sigma^{ij(k-1)} - \sum_{n=1}^{k-1}\sum_{l,m} P^{ijk:lmn}V^{lmn} = b$$

$$V^{ijk} = \frac{b}{(P^{000} + a\Delta t)}$$

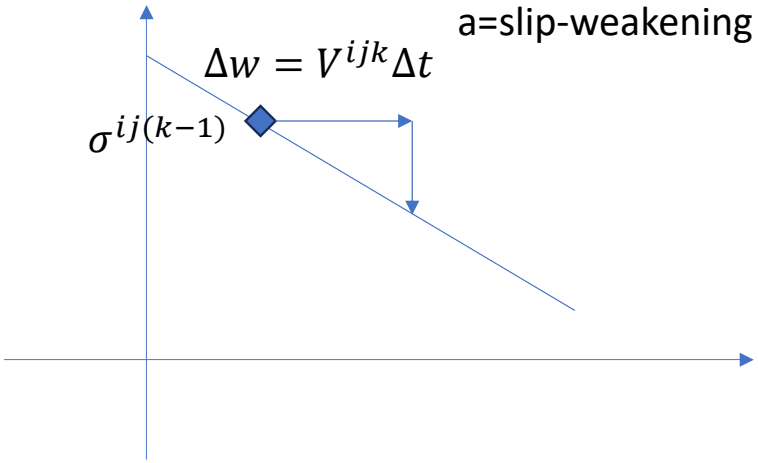

Numerical stability

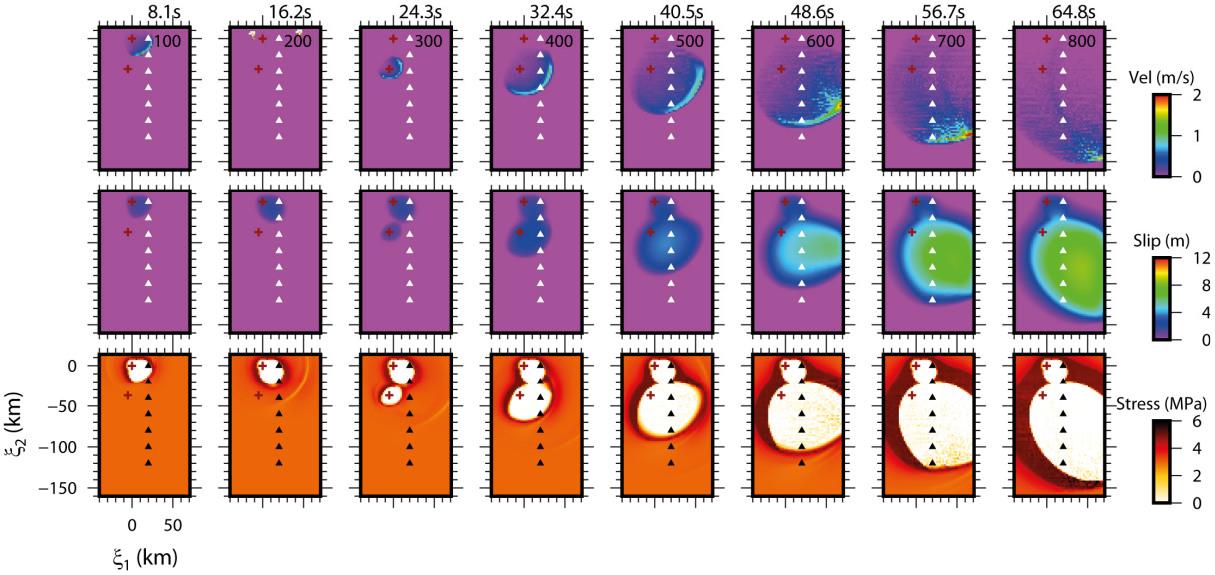

Figure S5: Snapshot (slip rate, slip and shear stress) of a simulation of rupture propagation with grid size Δs = 1.0 km and Δt = 0.081 s. See the caption of Figure S4.

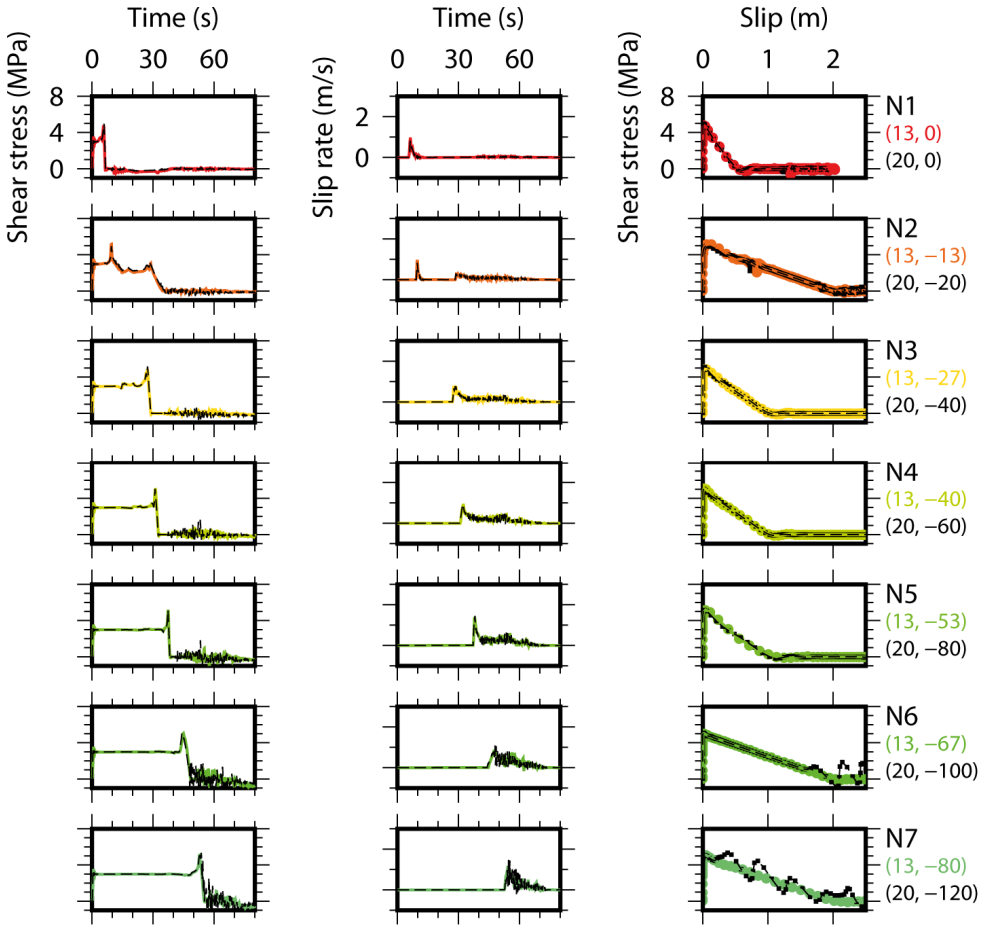

Figure S6: Comparison of two simulations presented in Figures S4 and S5 in terms of the temporal evolution of shear stress, slip rate and the slip-stress relation. The color lines indicate the case of Δs = 1.5 km (Figure S4) and the broken black lines are the one of Δs = 1.0 km (Figure S3).

Aochi & Ruiz (2021)

Problems

$$\tau^{ijk} = \underbrace{P^{000:000} V^{ijk}}_{\text{current time step}} + \underbrace{\sum_{n=1}^{k-1} \sum_{l,m} P^{ijk:lmn} V^{lmn}}_{\text{past history}}$$

- Computaiton time
- Errors

Digital filter (=smoothing)

$V_k; k = 1,2, \ldots\ldots, n$ Original time series

$\overline{V}_k; k = 1,2, \ldots\ldots, n$ Filtered time series

$$\overline{V}_1 = V_1$$
$$\overline{V}_k = S \cdot V_k + (1 - S) \cdot V_{k-1}; k \geq 2$$

$$0 < S \leq 1$$

Reference (forgotton…)

Further reading

- Cochard and Madaraiga (1994)
- Fukuyama and Madariaga (1995, 1998)
- Tada and Yamashita (1996)
- Kame and Yamashita(1998)
- Aochi (PhD thesis, 2000).